

Does incommensurability mean superlubricity?

Lukas Hörmann^{1,*}, Johannes J. Cartus¹, and Oliver T. Hofmann¹

¹Institute of Solid State Physics, Graz University of Technology, Petersgasse 16, 8010 Graz, Austria

*hoermann@tugraz.at

ABSTRACT

Friction is a major source of energy loss in mechanical devices. This energy loss may be minimised by creating interfaces with extremely reduced friction, i.e. superlubricity. Conventional wisdom holds that incommensurate interface structures facilitate superlubricity. However, despite the prevalence of incommensurate interfaces, most interfaces do not show notably low friction coefficients. In this study, we use a combination of density-functional theory and machine learning to investigate the mechanisms that lead to these large friction coefficients, and present design principles to engineer systems with particularly high or low friction coefficients.

Introduction

Friction causes a significant amount of energy consumption in any moving mechanical device. One way of reducing this energy loss is creating interfaces with extremely reduced friction, i.e. superlubricity. Superlubricity is a state of ultra-low friction, defined by a dynamic friction coefficient below 0.01.¹ Such low friction coefficients can be realized using control or actuation of the normal force,²⁻⁵ thermally activated drift,⁶⁻¹⁰ or structural superlubricity.¹¹⁻²⁰

Structural superlubricity^{1,21,22} is one of the most promising strategies to achieve ultra-low friction. This type of superlubricity relies on structural incommensurability, where the two surfaces (or a surface and an adsorbate) that meet at the sliding interface exhibit slightly different lattice spacings. Using the Frenkel-Kontorova model²³ it can be shown that for a surface with a lattice spacing of a and a rigid adsorbate with a lattice spacing of b lateral forces become infinitesimal beyond a critical value of a/b .²⁴ However, incommensurate structures are often subject to deformations that may be driven by the forces occurring during interfacial sliding,^{25,26} or are a result of phase transitions²⁷⁻³⁰ or static distortion waves.³¹⁻³⁵ We expect that these deformations strongly impact the frictional properties. This prompts the question, of whether it is possible to identify systems where incommensurate structures are stabilised and where robust structural superlubricity is maintained.

To this aim, we investigate the static friction coefficient of interfaces between metal substrates and molecular adlayers (organic/metal interfaces). The static friction coefficient is directly related to the maximal lateral force that occurs when two interfaces slide against each other. It is usually larger than the dynamic friction coefficient,³⁶ which is related to the dissipative forces during interfacial sliding. As a result, an ultra-low static friction coefficient implies superlubricity. Experimental examples for low static friction coefficients are for instance polytetrafluorethylene on polytetrafluorethylene with 4×10^{-2} , hard steel on hard steel, which exhibits 7.8×10^{-1} , or hard steel on graphite with 2.1×10^{-1} .³⁷

In organic/metal interface systems there exists a com-

plex relationship between the chemical compositions of the molecules and the substrate, the interplay of molecule-substrate and molecule-molecule interactions, the structure of the interface, and ultimately the frictional properties. A comprehensive understanding of this relationship is required to infer design principles for ultra-low friction. Recently it was demonstrated that the superlubric state of an incommensurate configuration of a graphene flake on graphite breaks down because the forces that act on the individual atoms lead to a rearrangement of the interface structure into a commensurate one.²⁶ Moreover, the impact of the sliding speed, sliding direction, temperature, and normal force has been studied for the same system.³⁸ However, both studies concentrated on a system consisting purely of carbon atoms and employed classical force field potentials. In fact, most theoretical works on nanoscale friction have focused on idealised systems and small unit cells,³⁹ which are too small to capture mesoscale phenomena such as static distortion waves, or have used classical force field methods,^{40,41} which do not account for quantum mechanical effects at the interface, such as charge transfer or the formation or breaking of bonds. We overcome these limitations by using state-of-the-art density functional theory (DFT) computations in conjunction with a machine-learned interatomic potential (MLIP) to determine energies and forces at sliding interfaces. Thereby we consider organic/metal interface systems that contain thousands to tens of thousands of atoms. By considering interfaces of this scale we push the boundaries of first principles studies on nanoscale friction to the previously inaccessible mesoscale. We demonstrate that is necessary to account for structural effects such as incommensurability and static distortion waves that govern friction.

We focus on two prototypical organic/metal interfaces: Naphthalene on Cu(111) and tetrachloropyrazine (TCP) on Pt(111). Naphthalene is a simple polycyclic aromatic hydrocarbon. It forms a variety of physisorbed adlayer structures on the Cu(111) surface. In experiment^{42,43} and theory⁴⁴ this system exhibits commensurate and incommensurate structures at various thermodynamic conditions. TCP is a heterocyclic aromatic organic molecule. On the Pt(111) surface TCP forms

chemisorbed and physisorbed adsorption states.⁴⁵ In an earlier work²⁷ we found strong evidence that chemisorbed TCP forms commensurate and physisorbed TCP forms incommensurate structures. The fact that both systems exhibit both commensurate and incommensurate structures allows us to study the dependence of the static friction coefficient on static distortion waves.

Results and discussion

As discussed in the introduction, structural superlubricity relies on the incommensurability of the interface. Whether commensurate or incommensurate structures form is governed by the balance of molecule-substrate interactions and molecule-molecule interactions.^{46,47} Strong molecule-molecule interactions and a comparatively weak corrugation of molecule-substrate interactions allow maximising the energy gain from interactions between molecules. This will most likely lead to incommensurate layers. Conversely, a large corrugation of molecule-substrate interactions and comparatively weak molecule-molecule interactions force the molecules to remain in energetically favourable adsorption sites. Any energy gain from favourable molecule-molecule interactions would be outweighed by the energy penalty from unfavourable molecule-substrate interactions. This leads to commensurate layers. Concurrently, in an incommensurate adlayer, the aforementioned delicate balance of interactions may change locally depending on the respective positions of adsorbate atoms and atoms of the molecule. This may lead to the formation of static distortion waves³¹⁻³⁵ which we expect to result in a breakdown of structural superlubricity.

In this paper, we investigate the connection between the interactions at the interface, the geometric structure and the frictional properties. For this we organise the Results Section as follows: First, we discuss the close-packed interface structures for which we determine static friction coefficients. Second, we investigate the emergence of incommensurability and static distortion waves as a result of the interplay between molecule-substrate and molecule-molecule interactions. Finally, we investigate the impact this has on the static friction coefficient and use our findings to formulate a design principle for superlubricating organic/metal interfaces.

Structures of continuous adlayers

To determine the static friction coefficient of naphthalene on Cu(111) and TCP on Pt(111) we must first know the interface structure(s) of both systems. Therefore, we identify the most energetically favourable structures of both materials. Thereby we consider both commensurate (one molecule per unit cell) and pseudo-incommensurate (in the order of hundred molecules per unit cell) structures. Truly incommensurate interfaces contain an infinite number of molecules per unit cell. Since each molecule has a different adsorption site the friction coefficient becomes 0.0 in this case. However, the electronic structure of an infinite number of molecules is impossible to calculate with first principles methods. There-

fore, we approximate incommensurate with large but finite (pseudo-incommensurate) unit cells that will exhibit a finite friction coefficient.

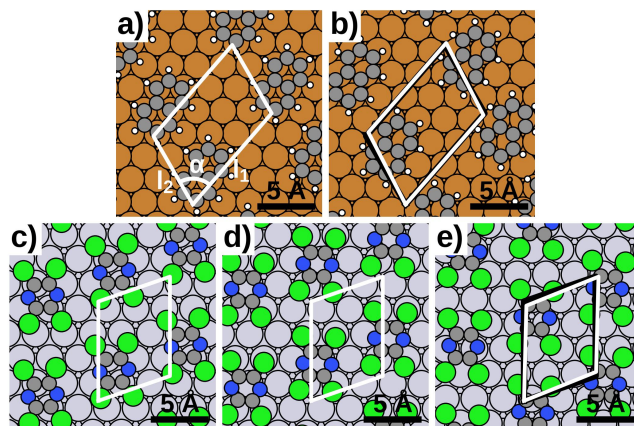


Figure 1. Close-packed adlayer structures used to calculate static friction coefficients; a) commensurate structure of naphthalene on Cu(111); b) incommensurate structure of naphthalene on Cu(111); c) commensurate structure of chemisorbed TCP on Pt(111); d) commensurate structure of physisorbed TCP on Cu(111); e) incommensurate structure of physisorbed TCP on Cu(111); unit cells are shown in white, for incommensurate structures (b, e) the unit cells of the respective commensurate structures (a, d) are shown in black; Lattice parameters are given below:

	l_1	l_2	α
a)	11.7 Å	7.6 Å	70.9°
b)	11.5 Å	7.9 Å	68.4°
c)	7.3 Å	9.6 Å	70.9°
d)	7.3 Å	9.6 Å	70.9°
e)	7.5 Å	9.2 Å	66.7°

In the case of naphthalene, we can make use of experimentally determined commensurate and incommensurate structures.^{42,43} Both structures exhibit a similar molecular orientation and only have slightly different molecular periodicities. We approximate the incommensurate structure with a pseudo-incommensurate structure containing 150 molecules per unit cell (see figure 1b). The commensurate structure contains 1 molecule per unit cell (see figure 1a).

In the case of TCP on Pt(111), we are not aware of an experimental structure determination. Therefore, we use theoretically determined structures based on the results from an earlier publication.²⁷ We select structures based on the most favourable energy per molecule. The energy per molecule is the appropriate measure since a sub-monolayer coverage is a good assumption in nanoscale friction experiments. To determine the energies and forces of all structures (also those of naphthalene on Cu(111)), we use an MLIP. As an improvement over the MLIP used in our previous publication²⁷ we now employ a descriptor based on the smooth overlap of atomic positions (SOAP)⁴⁸ instead of radial distance functions.

For the sake of consistency, we recalculate the formation energy for all structures. Details and a comparison between the MLIP and the old machine-learning models are given in the Methods Section and the Supporting Information.

As stated above, TCP forms chemisorbed and physisorbed structures on Pt(111). For the present study, we use the physisorbed structure with the most favourable formation energy per molecule, which is pseudo-incommensurate and contains 240 molecule per unit cell (see figure 1e). We obtain this structure by using a simulated-annealing-based global minimum search. This search reconfirms the findings of our earlier study²⁷, which has strongly indicated that the most favourable physisorbed structure is incommensurate. Additionally, we include a chemisorbed and physisorbed commensurate structure, both containing 1 molecule per unit cell as reference points in our study. The unit cells of these commensurate structures constitute the closest possible match compared to the one-molecule unit cell of the pseudo-incommensurate structure (see figure 1c and d). We note that our previous study²⁷ has shown that the most favourable chemisorbed structure of TCP on Pt(111) is commensurate.

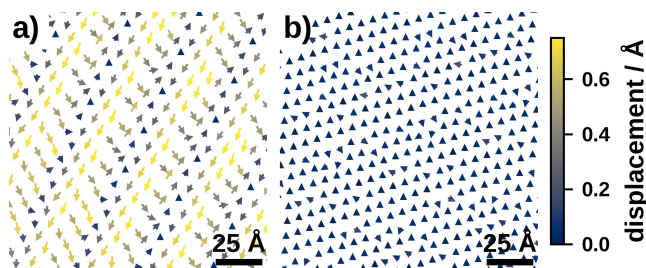


Figure 2. Displacement vectors between the molecules of the pseudo-incommensurate and optimised structures of a) naphthalene on Cu(111) and b) physisorbed TCP on Pt(111); displacement vectors are scaled by a factor of 5 and colour-coded for better visualisation.

So far we have only considered structures (commensurate and pseudo-incommensurate) where all molecules are neatly arranged on a grid. However, in the (pseudo-)incommensurate structures the molecules assume a great variety of different adsorption sites – some of which may be located on energetically unfavourable positions of the potential energy surface (PES) (see molecule-substrate interactions). Such molecules may move to assume more energetically favourable adsorption sites. Naturally, this will incur an energy penalty from unfavourable molecule-molecule interactions. Therefore, such deformations will only occur to the extent where the energy gains outweigh the penalties. We expect that deformations of a significant magnitude, such as static distortion waves, have a significant impact on the frictional properties of the interface. To investigate the occurrence of such deformations, we use our MLIP to conduct geometry optimisations (of the positions and orientations of the molecule) of all molecules in the pseudo-incommensurate structures (the lattice vectors remain fixed). We will hereafter refer to these optimised

pseudo-incommensurate structures as optimised structures. The structure of **naphthalene on Cu(111)** deforms significantly during the geometry optimisation and forms a static distortion wave, as shown in figure 2. Conversely, the pseudo-incommensurate structure of **physisorbed TCP on Pt(111)** remains largely unchanged. The reasons for these behaviours will be discussed in the next section.

Interactions of the molecules on the surface

To understand why naphthalene on Cu(111) forms static distortion waves and why TCP on Pt(111) does not, it is instructive to analyse the different interactions that determine the stability of an adlayer structure. The stability of adlayer structures on the metal substrate is determined by their formation energy, which we define as the difference between the combined interface system and the interface components (see Methods Section). The formation energy can be decomposed into molecule-substrate and the molecule-molecule interactions,^{44,46,47} which we will analyse in the next two subsections.

Molecule-substrate interactions The molecule-substrate interactions can be described by the PES of an isolated molecule on the substrate. The PES not only yields insight into the formation of possible adlayer structures, but it contains a good approximation of the potential barrier an individual molecule has to overcome during interfacial sliding. We determine the PES using the MLIP. Thereby we coarse-grain the PES (see Methods Section) and concentrate on the most important degrees of freedom: These are the x , y and z coordinate of the centre of mass of the molecule, as well as orientation (around the z axis) and the bending (only in the case of chemisorbed TCP) of the molecule. The algorithm uses DFT-calculated energies of 50 to 80 adsorption geometries as input and interpolates between them. Details about this approach and the accuracy of the prediction can be found in the Methods Section and the Supporting Information.

Figure 3 shows the x and y dimensions of the PESs for naphthalene on Cu(111) as well as TCP on Pt(111). To determine this 2-dimensional cross-section of the PES we chose molecular orientations that match the orientation of the molecules in the energetically most favourable close-packed adlayers (see figure 1). For the height z and the bending, we chose the energetically most favourable coordinates. **Naphthalene on Cu(111)** is physisorbed and the molecular backbone remains planar. The corrugation of the molecule-substrate interaction of naphthalene on Cu(111) amounts to approximately 0.2 eV.

TCP on Pt(111) can either be chemisorbed or physisorbed. The molecule-substrate interactions of **chemisorbed TCP on Pt(111)** exhibit a corrugation of approximately 2.0 eV, as we have already shown in our previous work.²⁷ This is a result of (A) the formation of (site-specific) covalent bonds with the substrate and (B) the strong distortion of the molecular geometry. Conversely, **physisorbed TCP on Pt(111)** remains flat and the corrugation of the PES is only 0.04 eV. Notably, this is one order of magnitude smaller than the corrugation of

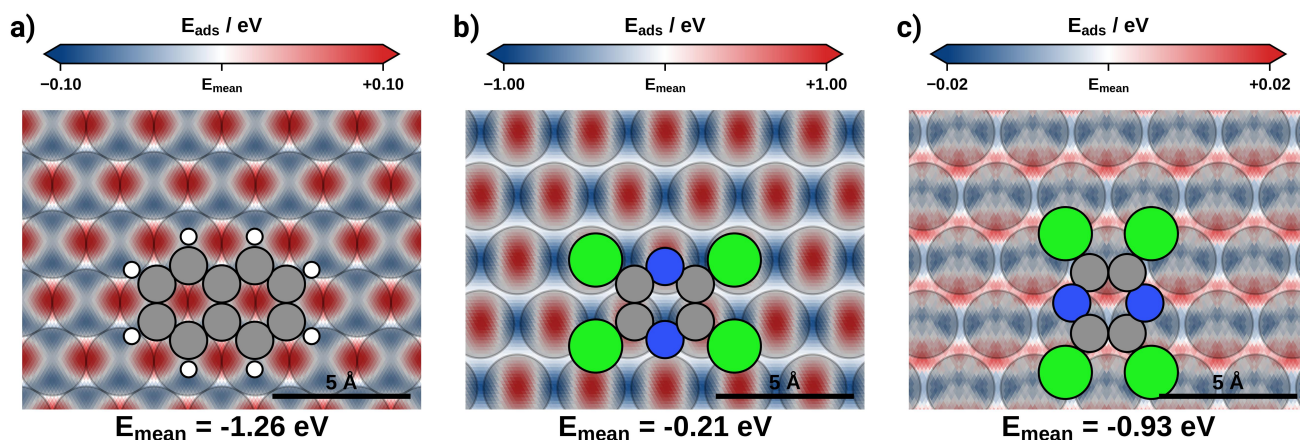


Figure 3. PES of individual molecules; a) PES of naphthalene; b) PES of chemisorbed TCP; c) PES of physisorbed TCP; The PESs shown represent 2-dimensional (x, y) cross sections of the 4-dimensional (naphthalene and physisorbed TCP) or the 5-dimensional (chemisorbed TCP) PES - the molecular orientations matches the orientation of the molecules in the energetically most favourable close-packed adlayers and the energetically most favourable coordinate is chosen; Energies shown are relative to the E_{mean} indicated at the bottom of each subfigure; For clarity on the first layer of the substrate is shown;

naphthalene on Cu(111).

Molecule-molecule interactions As mentioned earlier, the formation of a given interface structure is governed by a balance between the molecule-substrate and the molecule-molecule interactions. To determine the molecule-molecule interactions, we place a pair of molecules (in isolation) onto the surface. The first molecule is kept fixed while the second one is placed at different x and y positions neighbouring the first molecule. For the height z we choose the mean adsorption height and molecular orientations reflecting the orientation of the molecules in the energetically most favourable close-packed adlayers (similar to figure 3). For each position of the second molecule, we determine the formation energy and subtract the molecule-substrate interaction of both molecules. Figure 4 shows the molecule-molecule interactions for naphthalene on Cu(111) and TCP on Pt(111).

Naphthalene on Cu(111) exhibits exclusively repulsive molecule-molecule interactions, which become nearly zero outside the zone of Pauli-pushback. If the H-atoms of two molecules are further apart than 1.0 \AA , the interaction energies are equal to or smaller than 0.2 eV . Adlayer structures with more closely packed molecules are thus energetically unfavourable. The fact that naphthalene has small and uniform molecule-molecule interactions would commonly indicate that its adlayers are commensurate. However, whether a commensurate or an incommensurate adlayer forms depends on the relative strength of the molecule-substrate and the molecule-molecule interactions. The molecule-substrate interactions have an equally weak corrugation of approximately 0.2 eV . This explains why naphthalene adlayers form commensurate as well as incommensurate structures in experiment.^{42,43} **Chemisorbed TCP on Pt(111)** also exhibits

largely repulsive molecule-molecule interactions (Figure 4b). The energies lie within a range of -0.2 eV to 0.2 eV . Since the molecule-substrate interactions of chemisorbed TCP feature a corrugation of 2.0 eV that is approximately an order of magnitude larger than the molecule-molecule interactions, chemisorbed adlayers are commensurate, as shown in our previous publication.²⁷ **Physisorbed TCP on Pt(111)** shows regions of repulsive and attractive molecule-molecule interactions. The interaction energies are comparable in size to those of chemisorbed TCP (-0.2 eV to 0.2 eV). Notably, attractive molecule-molecule interactions of approximately 0.1 eV can be observed when Cl- and N-atoms are in close proximity (this configuration is indicated in figure 4b). These attractive molecule-molecule interactions in conjunction with the very small corrugation of the molecule-substrate interactions likely lead to a stabilisation of (pseudo-)incommensurate adlayers.

The connection of superlubricity and incommensurability

In discussions about structural superlubricity, one often finds the general statement, that incommensurate structures lead to vanishing lateral forces and, hence, facilitate superlubricity.¹ While it is true that a perfectly incommensurate interface would lead to superlubricity, real systems (including the ones discussed here) may form static distortion waves. We gauge the impact of these distortions on the frictional properties by comparing the following structures: (A) We take commensurate structures of naphthalene on Cu(111) as well as chemisorbed and physisorbed TCP on Pt(111) as a reference point for the static friction coefficient. (B) We investigate perfectly pseudo-incommensurate (identical spacing for all molecules) structures of naphthalene on Cu(111) and physisorbed TCP on Pt(111) to determine a lower boundary

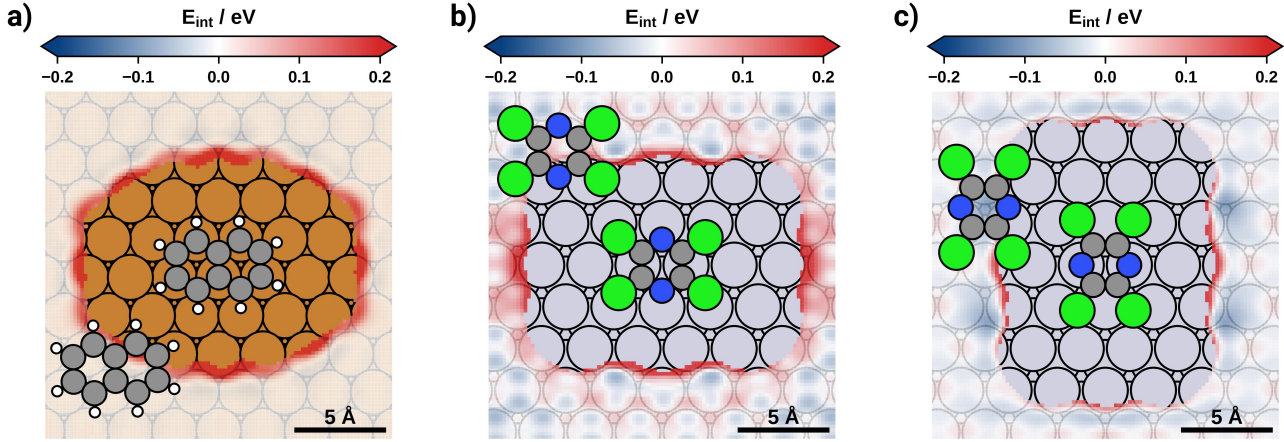


Figure 4. Molecule-molecule interactions; a) naphthalene on Cu(111); b) TCP in the chemisorbed state; c) TCP in the physisorbed state.

for the friction coefficients. These pseudo-incommensurate structures closely match the commensurate structures to allow a direct comparison. (C) We analyse optimised structures of naphthalene on Cu(111) and physisorbed TCP on Pt(111), that is pseudo-incommensurate structures whose molecular x , y and z coordinates as well as orientations were allowed to relax and to form – in case of naphthalene – static distortion waves.

To determine the static friction coefficient, we shift the different molecular adlayers across the surface. The paths are given by the primitive substrate lattice vector of the (111)-surface. The different directions (hereafter called primitive directions) are indicated in figure 5. We note in passing that opposite directions appear symmetric due to substrate symmetries, but are strictly not symmetric due to the adsorbate layer. At equidistant points along these paths, we determine adsorption energies and forces acting on the adlayer using the MLIP. Thereby we apply a normal force individually to all molecules in the unit cell. To find the equilibrium adsorption height of each molecule the z coordinate of its centre of mass is optimised (under the impact of the vertical force) using the MLIP. We convert the vertical forces into vertical pressures for a clear representation in figure 5. The range of vertical pressures from 0.001 GPa to 0.1 GPa reflects experimentally used pressures.^{1,20}

The lateral force is a result of the interfacial PES (molecule-substrate plus molecule-molecule interactions). Its maximum value opposite the shear direction (i.e. when moving “up” an energy barrier) directly relates to the static friction coefficient. The friction coefficient can be determined from the relationship of the lateral force F_x and the respective normal force F_z :

$$\mu_s = \frac{1}{F_z} \max(F_x) \quad (1)$$

Figures 5 and 6 present a comparison of the static friction coefficients of naphthalene and TCP respectively. Thereby we compare commensurate, pseudo-incommensurate and optimised structures.

Commensurate **naphthalene on Cu(111)** exhibits large static friction coefficients of approximately 5×10^0 to 5×10^2 that are isotropic in all 6 primitive directions of the 111-surface (see figure 6). Conversely, the pseudo-incommensurate adlayer of naphthalene displays a strongly anisotropic static friction coefficient. In $[0, 1, \bar{1}]$ - and $[0, \bar{1}, 1]$ -direction it has a static friction coefficient of approximately 2×10^{-2} to 5×10^{-1} that is nearly 3 orders of magnitude smaller than that of the commensurate adlayer. In the other directions, the friction coefficients are comparable to the commensurate naphthalene structure. The reason for this can be gleaned from the PES of the molecule-substrate interaction in figure 3a: In $[0, 1, \bar{1}]$ -direction and $[0, \bar{1}, 1]$ -direction there are “grooves” in the PES along which the molecule can move without encountering large barriers. In the other two primitive directions, the barriers are higher, leading to a higher static friction coefficient. The optimised structure forms static distortion waves and exhibits a static friction coefficient comparable to the commensurate adlayer.

Chemisorbed TCP on Pt(111) has a very large static friction coefficient, with lateral forces being larger than the vertical force. We note that we did not allow for the sliding of the atoms of the metal substrate, which may in the case of chemisorbed TCP offer less resistance to lateral movement. Conversely, commensurate physisorbed adlayers show significantly lower static friction coefficients of approximately 0.9×10^0 to 1.2×10^2 , which are 2 orders of magnitude smaller than in the chemisorbed adlayer. In both cases, the friction coefficients are largely isotropic. Notably, commensurate adlayers of TCP have a static friction coefficient that is half an order of magnitude smaller than that of commensurate

static friction coefficient

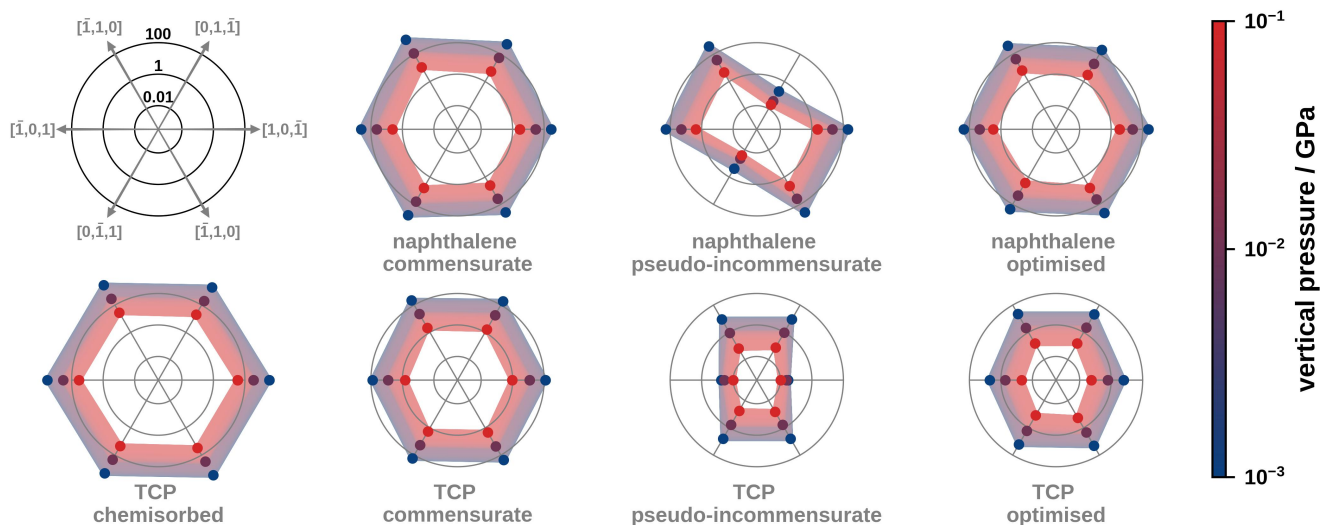


Figure 5. Dependence of the static friction coefficients for different structures of naphthalene on Cu(111) and TCP on Pt(111) on the direction of displacement; the solid dots in the plot indicate calculated static friction coefficients while the shaded area is an interpolation which should serve as a guide for the eye

adlayers of naphthalene. This is a result of the small corrugation of the molecule-substrate interaction, which is 1 order of magnitude smaller than that of naphthalene on Cu(111). The pseudo-incommensurate adlayer of physisorbed TCP exhibits anisotropic static friction coefficients, with the minimum of 1.0×10^{-2} to 0.3×10^{-1} being found in the $[1, 0, \bar{1}]$ - and $[\bar{1}, 0, 1]$ -direction. These results are comparable to those of a pseudo-incommensurate adlayer of naphthalene. Compared to that the static friction coefficient of the optimised structure is minimally larger (5.0×10^{-2} to 6.0×10^0) and the directional dependence becomes isotropic. This friction coefficient is 2 orders of magnitude smaller than that of the commensurate adlayer of physisorbed TCP. Importantly, the static friction coefficient of the pseudo-incommensurate and the optimised structure differ by only half an order of magnitude, which is significantly smaller compared to the difference of more than two orders of magnitude we find for naphthalene on Cu(111). This is because the formation of static distortion waves in pseudo-incommensurate adlayers of TCP is suppressed by attractive molecule-molecule interactions, in contrast to naphthalene adlayers, where molecule-substrate interactions are dominant.

In summary, we find a strong impact of the type of commensurability on the static friction coefficient. As expected, pseudo-incommensurate structures exhibit ultra-low friction. Lower friction coefficients could in principle be computationally obtained with structures containing even more molecules per unit cell, but we do not expect that larger unit cell sizes impact the likelihood of the formation of static distortion waves. Static distortion waves cause a significant increase in friction. The formation of incommensurate organic/metal interfaces requires a physisorbed state since chemisorbed molecules

are usually strongly bonded to a specific site on the substrate. Moreover, static distortion waves may occur if the molecule-molecule interactions are small compared to the molecule-substrate interaction, as is the case for naphthalene on Cu(111). The stabilisation of an incommensurate adlayer requires strongly corrugated molecule-molecule interaction that leads to distinguished molecular arrangement, as is the case in physisorbed TCP.

Conclusion

In conclusion, the common statement that structural incommensurability implies superlubricity¹ must be taken with some caution. Although perfectly incommensurate structures indeed facilitate superlubricity, real systems are susceptible to structural distortions and symmetry breaking, which can significantly affect their frictional properties. In this study, we investigate two exemplary organic/metal interfaces: naphthalene on Cu(111) and TCP on Pt(111). Naphthalene on Cu(111) is physisorbed while TCP on Pt(111) can be either physisorbed or chemisorbed. We compare static friction coefficients of (A) commensurate, (B) pseudo-incommensurate and (C) geometry-optimised pseudo-incommensurate adlayer structures of both interfaces. We find that the optimised pseudo-incommensurate structure of naphthalene on Cu(111) exhibits static distortion waves leading to a static friction coefficient of similar magnitude as in commensurate structures. This is a result of dominant molecule-substrate interactions compared to the molecule-molecule interactions. Conversely, pseudo-incommensurate structures of TCP on Pt(111) are stabilised by strongly corrugated molecule-molecule interactions. Therefore, the pseudo-incommensurate structure of TCP on

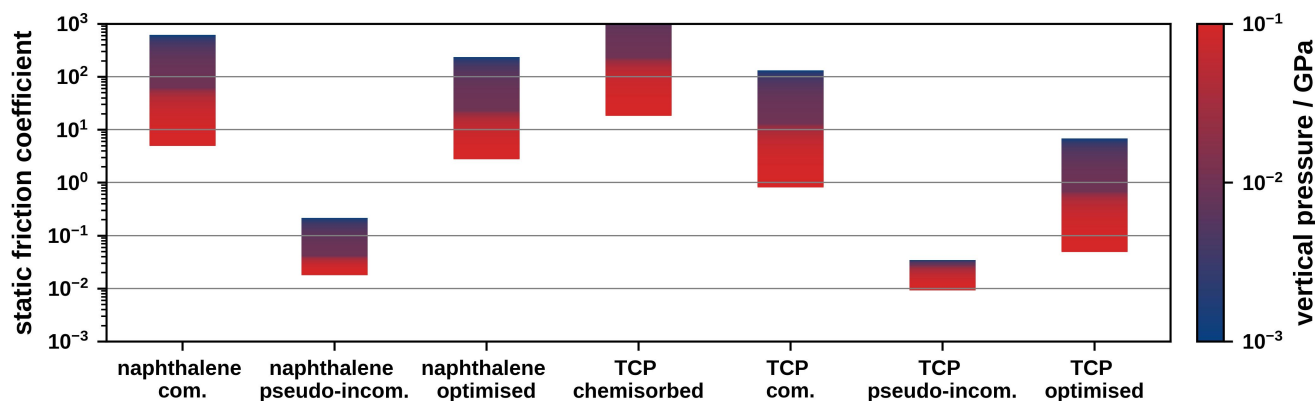


Figure 6. Comparison of static friction coefficients for different structures of naphthalene on Cu(111) and TCP on Pt(111)

Pt(111) displays a static friction coefficient that is approximately 2 orders of magnitude smaller than that of naphthalene on Cu(111). Based on these results we can formulate design principles to produce organic/metal interface systems that display superlubricity: (A) The formation of incommensurate structures requires relatively uniform molecule-substrate interactions, which are commonly only found in physisorbed systems. (B) Perfectly incommensurate structures, which (potentially) exhibit superlubricity, are geometrically stabilised in systems with strongly corrugated molecule-molecule interactions. On this basis, we may now answer the question posed in the title of this work: In organic/inorganic interface systems, incommensurability implies ultra-low friction only in systems where the molecule-molecule interactions dominate the formation of the interface structure.

Methods

Density functional theory calculations

Computational data is reused from previous work: (A) Data for naphthalene on Cu(111) comes from *SAMPLE: Surface structure search enabled by coarse-graining and statistical learning*⁴⁴ and (B) data for TCP on Pt(111) is taken from *From a bistable adsorbate to a switchable interface: tetrachloropyrazine on Pt (111)*.²⁷ The data are openly available in the NOMAD repository at [doi:10.17172/NOMAD/2023.05.01-1](https://doi.org/10.17172/NOMAD/2023.05.01-1) and [doi:10.17172/NOMAD/2022.03.15-1](https://doi.org/10.17172/NOMAD/2022.03.15-1). Information about convergence tests and computational settings can be found in our earlier publications. Similarly to these works, we determine the formation energy E_{form} of a structure from the difference between the energy of the adsorbed system E_{sys} and the energy of the pristine substrate E_{sub} as well as the energy of the relaxed molecule in vacuum E_{mol} multiplied by the number of molecules in the unit cell N .

$$E_{\text{form}} = E_{\text{sys}} - E_{\text{sub}} - N \cdot E_{\text{mol}} \quad (2)$$

Machine-learned interatomic potential

Determining static friction coefficients requires a large number of energy and force evaluations. The high computational cost associated with this prohibits the sole use of first-principles calculations. Therefore, we employ MLIP based on Gaussian process regression and the SOAP⁴⁸ descriptor to efficiently determine the energies and forces that are necessary to calculate the static friction coefficient. To train these MLIPs we use the energies and forces determined with first principles computations. Separate MPLIs are used for the individual systems: (A) Naphthalene on Cu(111), (B) physisorbed TCP on Pt(111) and (C) chemisorbed TCP on Pt(111). All MLIPs are trained to achieve a leave-one-out-cross-validation-room-mean-square-error (LOOCV-RMSE) that is smaller than chemical accuracy, i.e. 40 meV per molecule or 1 kcal mol⁻¹ on the training set. The LOOCV-RMSEs for all MLIPs are shown in the Supporting Information.

To improve the efficiency of the approach we employ a two-step approach: In the first step, we determine an approximate model for the formation energy $E_{\text{form}}^{\text{approx}}$. We split this approximate formation energy into a contribution from the molecule-substrate interaction and one from the molecule-molecule interaction:

$$E_{\text{form}}^{\text{approx}} = \sum_i E_{\text{mol-sub}}^i + E_{\text{mol-mol}} \quad (3)$$

The molecule-substrate interaction is calculated from the sum of molecule-substrate interactions of an isolated molecule on the surface $E_{\text{mol-sub}}^i$. To determine $E_{\text{mol-sub}}^i$ we train an MLIP to predict the PES of a single isolated molecule on the substrate (see figure 3). For the molecule-molecule interactions $E_{\text{mol-mol}}$ we use two different approaches. In the case of physisorbed TCP on Pt(111), we train an MLIP on energies of free-standing layers of molecule in vacuum (i.e. adlayer structures whose substrate was removed). This gives an approximate value for the molecule-molecule interaction (often called monolayer formation energy). This allows us to produce training data for large unit cells which could not

be calculated if the substrate were included. However, the molecule-molecule interaction may be altered significantly due to interactions with the substrate, such as charge transfer or molecular deformations.^{27,44} This is the case for naphthalene on Cu(111) and chemisorbed TCP on Pt(111), where the interactions change qualitatively. For this reason, it is more accurate to assume non-interacting molecules ($E_{\text{mol-mol}} = 0$) in the first learning step.

In a second step, we learn the residual ΔE_{form} resulting from predictions of adsorbed adlayers and the respective DFT calculations.

$$\Delta E_{\text{form}} = E_{\text{form}}^{\text{approx}} - E_{\text{form}} \quad (4)$$

This two-step procedure allows (A) using large unit cells in the first step to learn molecule-molecule interactions of higher commensurate adlayers and (B) learning the influence of the substrate in the second step. This enables us to consider adlayer structures with hundreds of molecules per unit cell.

Computational structure determination

To determine the most energetically favourable pseudo-incommensurate structure of TCP on Pt(111) we perform global optimisation using a Metropolis algorithm. This approach is reminiscent of the simulated annealing optimization we used in a previous publication⁴⁴. For the current work, the Metropolis algorithm allows us to more efficiently sample structures containing up to 400 molecules per unit cell: The Metropolis algorithm chooses a new pseudo-incommensurate structure (with new lattice parameters) and directly evaluates its formation energy $E_{\text{form}}(x_{i+1})$. The new structure is accepted based on the following equation, where $E_{\text{form}}(x_i)$ is the energy of the previous structure:

$$p = \min \left(1, \exp \left(\frac{E_{\text{form}}(x_i) - E_{\text{form}}(x_{i+1})}{k_B T} \right) \right) \quad (5)$$

Unlike our earlier simulated annealing optimisation, the Metropolis algorithm does not perform full local geometry optimisation on each pseudo-incommensurate structure. Forgoing these optimisations is merited in the case of TCP on Pt(111), since the energy gained through geometry optimisation is in the meV-range, i.e. pseudo-incommensurate structures of TCP on Pt(111) are already energetically and geometrically very close to the respective optimised structure. Based on the results of the Metropolis algorithm, we optimise the most energetically favourable pseudo-incommensurate structures. Thereby we optimise the x , y , z coordinate and orientation around the z axis of each of the hundreds of molecules in the structure using a Broyden-Fletcher-Goldfarb-Shanno algorithm.⁴⁹⁻⁵²

Data availability

The data supporting this research are openly available in the NOMAD repository at doi:10.17172/NOMAD/2023.05.01-1 and doi:10.17172/NOMAD/2022.03.15-1.

References

1. Baykara, M. Z., Vazirisereshk, M. R. & Martini, A. Emerging superlubricity: A review of the state of the art and perspectives on future research. *Appl. Phys. Rev.* **5**, 041102 (2018).
2. Socoliuc, A., Bennewitz, R., Gnecco, E. & Meyer, E. Transition from stick-slip to continuous sliding in atomic friction: Entering a new regime of ultralow friction. *Phys. Rev. Lett.* **92**, 134301, DOI: [10.1103/PhysRevLett.92.134301](https://doi.org/10.1103/PhysRevLett.92.134301) (2004).
3. Medyanik, S. N., Liu, W. K., Sung, I.-H. & Carpick, R. W. Predictions and observations of multiple slip modes in atomic-scale friction. *Phys. Rev. Lett.* **97**, 136106, DOI: [10.1103/PhysRevLett.97.136106](https://doi.org/10.1103/PhysRevLett.97.136106) (2006).
4. Socoliuc, A. *et al.* Atomic-scale control of friction by actuation of nanometer-sized contacts. *Science* **313**, 207–210 (2006).
5. Gnecco, E. *et al.* Dynamic superlubricity on insulating and conductive surfaces in ultra-high vacuum and ambient environment. *Nanotechnology* **20**, 025501 (2008).
6. Krylov, S. Y., Jinesh, K. B., Valk, H., Dienwiebel, M. & Frenken, J. W. M. Thermally induced suppression of friction at the atomic scale. *Phys. Rev. E* **71**, 065101, DOI: [10.1103/PhysRevE.71.065101](https://doi.org/10.1103/PhysRevE.71.065101) (2005).
7. Jinesh, K. B., Krylov, S. Y., Valk, H., Dienwiebel, M. & Frenken, J. W. M. Thermolubricity in atomic-scale friction. *Phys. Rev. B* **78**, 155440, DOI: [10.1103/PhysRevB.78.155440](https://doi.org/10.1103/PhysRevB.78.155440) (2008).
8. Steiner, P. *et al.* Two-dimensional simulation of superlubricity on nacl and highly oriented pyrolytic graphite. *Phys. Rev. B* **79**, 045414, DOI: [10.1103/PhysRevB.79.045414](https://doi.org/10.1103/PhysRevB.79.045414) (2009).
9. Perez, D., Dong, Y., Martini, A. & Voter, A. F. Rate theory description of atomic stick-slip friction. *Phys. Rev. B* **81**, 245415, DOI: [10.1103/PhysRevB.81.245415](https://doi.org/10.1103/PhysRevB.81.245415) (2010).
10. Dienwiebel, M. *et al.* Superlubricity of graphite. *Phys. Rev. Lett.* **92**, 126101, DOI: [10.1103/PhysRevLett.92.126101](https://doi.org/10.1103/PhysRevLett.92.126101) (2004).
11. Liu, Z. *et al.* Observation of microscale superlubricity in graphite. *Phys. Rev. Lett.* **108**, 205503 (2012).
12. Zhang, R. *et al.* Superlubricity in centimetres-long double-walled carbon nanotubes under ambient conditions. *Nat. Nanotechnol.* **8**, 912–916 (2013).
13. Song, Y. *et al.* Robust microscale superlubricity in graphite/hexagonal boron nitride layered heterojunctions. *Nat. Mater.* **17**, 894–899 (2018).
14. Cihan, E., Ipek, S., Durgun, E. & Baykara, M. Z. Structural lubricity under ambient conditions. *Nat. Commun.* **7**, 1–6 (2016).

15. Benassi, A., Ma, M., Urbakh, M. & Vanossi, A. The breakdown of superlubricity by driving-induced commensurate dislocations. *Sci. Rep.* **5**, 1–13 (2015).
16. Ma, M., Benassi, A., Vanossi, A. & Urbakh, M. Critical length limiting superlow friction. *Phys. Rev. Lett.* **114**, 055501 (2015).
17. Sharp, T. A., Pastewka, L. & Robbins, M. O. Elasticity limits structural superlubricity in large contacts. *Phys. Rev. B* **93**, 121402 (2016).
18. Berman, D., Deshmukh, S. A., Sankaranarayanan, S. K., Erdemir, A. & Sumant, A. V. Macroscale superlubricity enabled by graphene nanoscroll formation. *Science* **348**, 1118–1122 (2015).
19. Berman, D. *et al.* Operando tribochemical formation of onion-like-carbon leads to macroscale superlubricity. *Nat. Commun.* **9**, 1–9 (2018).
20. Liu, S.-W. *et al.* Robust microscale superlubricity under high contact pressure enabled by graphene-coated microsphere. *Nat. Commun.* **8**, 1–8 (2017).
21. Hirano, M. & Shinjo, K. Atomistic locking and friction. *Phys. Rev. B* **41**, 11837 (1990).
22. Shinjo, K. & Hirano, M. Dynamics of friction: superlubric state. *Surf. Sci.* **283**, 473–478 (1993).
23. Kontorova, T. & Frenkel', Y. K teoriiy plastychnoyi deformatsiyi ta podviynosti. *Zh. Eksp. Teor. Fiz.* **8**, 89 (1938).
24. Peyrard, M. & Aubry, S. Critical behaviour at the transition by breaking of analyticity in the discrete frenkel-kontorova model. *J. Phys. C: Solid State Phys.* **16**, 1593 (1983).
25. Filippov, A. E., Dienwiebel, M., Frenken, J. W., Klafter, J. & Urbakh, M. Torque and twist against superlubricity. *Phys. Rev. Lett.* **100**, 046102 (2008).
26. de Wijn, A. S., Fusco, C. & Fasolino, A. Stability of superlubric sliding on graphite. *Phys. Rev. E* **81**, 046105, DOI: [10.1103/PhysRevE.81.046105](https://doi.org/10.1103/PhysRevE.81.046105) (2010).
27. Hörmann, L., Jeindl, A. & Hofmann, O. T. From a bistable adsorbate to a switchable interface: tetrachloropyrazine on pt (111). *Nanoscale* **14**, 5154–5162 (2022).
28. Panich, A., Mogilyansky, D. & Sardarly, R. Phase transitions and incommensurability in the layered semiconductor tlns2—an nmr study. *J. Phys. Condens. Matter.* **24**, 135901 (2012).
29. Stephens, P. W. *et al.* High-resolution x-ray-scattering study of the commensurate-incommensurate transition of monolayer kr on graphite. *Phys. Rev. B* **29**, 3512 (1984).
30. Kilian, L. *et al.* The commensurate-to-incommensurate phase transition of an organic monolayer: A high resolution leed analysis of the superstructures of ntcd a on ag (1 1 1). *Surf. Sci.* **602**, 2427–2434 (2008).
31. Novaco, A. D. & McTague, J. P. Orientational epitaxy—the orientational ordering of incommensurate structures. *Phys. Rev. Lett.* **38**, 1286 (1977).
32. Novaco, A. D. Theory of orientational epitaxy in the self-consistent phonon approximation. *Phys. Rev. B* **19**, 6493 (1979).
33. McTague, J. & Novaco, A. Substrate-induced strain and orientational ordering in adsorbed monolayers. *Phys. Rev. B* **19**, 5299 (1979).
34. Novaco, A. D. Theory of the structure and lattice dynamics of incommensurate solids: A classical treatment. *Phys. Rev. B* **22**, 1645 (1980).
35. Meissner, M. *et al.* Flexible 2d crystals of polycyclic aromatics stabilized by static distortion waves. *ACS Nano* **10**, 6474–6483 (2016).
36. Huang, J. Y. Coefficients of friction: Static versus dynamic. In *ASME/IEEE Joint Rail Conference*, vol. 83587, V001T03A001 (American Society of Mechanical Engineers, 2020).
37. Barrett, R. T. Fastener design manual. Tech. Rep. (1990).
38. Filippov, A. E., Dienwiebel, M., Frenken, J. W. M., Klafter, J. & Urbakh, M. Torque and twist against superlubricity. *Phys. Rev. Lett.* **100**, 046102, DOI: [10.1103/PhysRevLett.100.046102](https://doi.org/10.1103/PhysRevLett.100.046102) (2008).
39. Wang, J. *et al.* Theoretical study of superlow friction between two single-side hydrogenated graphene sheets. *Tribol. Lett.* **48**, 255–261 (2012).
40. Samadashvili, N., Reischl, B., Hynninen, T., Ala-Nissilä, T. & Foster, A. Atomistic simulations of friction at an ice-ice interface. *Friction* **1**, 242–251 (2013).
41. Falk, K., Sedlmeier, F., Joly, L., Netz, R. R. & Bocquet, L. Molecular origin of fast water transport in carbon nanotube membranes: superlubricity versus curvature dependent friction. *Nano Lett.* **10**, 4067–4073 (2010).
42. Yamada, T. *et al.* Novel growth of naphthalene overlayer on cu (111) studied by stm, leed, and 2ppe. *J. Phys. Chem. C* **114**, 13334–13339 (2010).
43. Forker, R. *et al.* The complex polymorphism and thermodynamic behavior of a seemingly simple system: naphthalene on cu (111). *Langmuir* **30**, 14163–14170 (2014).
44. Hörmann, L., Jeindl, A., Egger, A. T., Scherbela, M. & Hofmann, O. T. Sample: Surface structure search enabled by coarse graining and statistical learning. *Comput. Phys. Commun.* **244**, 143–155 (2019).
45. Liu, W., Filimonov, S. N., Carrasco, J. & Tkatchenko, A. Molecular switches from benzene derivatives adsorbed on metal surfaces. *Nat. Commun.* **4**, 1–6 (2013).
46. Hooks, D. E., Fritz, T. & Ward, M. D. Epitaxy and molecular organization on solid substrates. *Adv. Mater.* **13**, 227–241 (2001).

47. Mannsfeld, S. & Fritz, T. Understanding organic–inorganic heteroepitaxial growth of molecules on crystalline substrates: Experiment and theory. *Phys. Rev. B* **71**, 235405 (2005).
48. Bartók, A. P., Kondor, R. & Csányi, G. On representing chemical environments. *Phys. Rev. B* **87**, 184115 (2013).
49. Broyden, C. G. The convergence of a class of double-rank minimization algorithms 1. general considerations. *IMA J. Appl. Math.* **6**, 76–90 (1970).
50. Fletcher, R. A new approach to variable metric algorithms. *Comput. J.* **13**, 317–322 (1970).
51. Goldfarb, D. A family of variable-metric methods derived by variational means. *Math. Comput.* **24**, 23–26 (1970).
52. Shanno, D. F. Conditioning of quasi-newton methods for function minimization. *Math. Comput.* **24**, 647–656 (1970).

Acknowledgements

Financial support by the UFO grant of the Land Steiermark via the project “Schaltbare Superschmierfähigkeit” (SNIC: 416) is gratefully acknowledged by L.H. JJC and OTH gratefully acknowledge financial support from the Austrian Science Fund (FWF) via the project Y1157-N36 “MAP-DESIGN”. Computational results have been achieved using the Vienna Scientific Cluster (VSC).

Author contributions statement

L.H. conceived the research idea, carried out the simulations and data analysis and wrote the manuscript, J.J.C. helped to analyse the data and helped to edit the manuscript. O.T.H. supervised the research and helped to edit the manuscript. All authors reviewed the manuscript.

Conflicts of interest

The authors declare no competing interests.